Moroccan Journal of Chemistry
ISSN: 2351-812X
http://revues.imist.ma/?journal=morjchem&page=login
Tabaghat & al. / Mor. J. Chem. 7 N°4 (2019) 595-614

Grafting of fibrillated cellulose with acrylic compounds: Synthesis, Properties and Biodegradation

Tabaght Fatima Ezahra[1], El Idrissi Abderrahmane[1], Achelhi Nafea[1], Elyousfi Redouane[1], Bellaouchi Reda[2], Asehraou Abdeslam[2], Soufian Elbarkany[3].

1. Laboratory Applied chemistry and environmental (LCAE-URAC18), Mohammed first University, Faculty of Sciences, Oujda 60000, Morocco
2. Laboratory of Biochemistry and Biotechnology, Mohammed first University, Faculty of Sciences, Oujda 60000, Morocco
3. Laboratory of Applied Chemistry and Environment, Mohammed first University, Multidisciplinary Faculty of Nador 62000, Morocco

** Corresponding author:*
f.tabaght@ump.ac.ma
Received 08 Jun 2019,
Revised 25 sept 2019,
Accepted 03 Oct 2019

Abstract

The cellulose and cellulose acetate (CA) have been directly grafted with an acrylic compounds using a grafting to method with a free isocyanate group as a coupling agent in homogeneous medium. The grafting reaction parameters were optimized compared to grafting reaction in heterogeneous conditions. The grafted products (Cell-RSH, Cell-R'SH, CA-RSH and CA-R'SH) with well-defined architecture were characterized by FTIR, ^{1}H NMR and ^{13}C NMR, their thermal degradation was also studied by thermal analysis (TGA/ DTG). The effect of solvent systems on their solubility behavior was also investigated. The biodegradation process of these derivatives was established using two different procedures. The introduction of different side chain lengths and nature groups with well-defined architecture into the main chain of cellulose and CA can modify their phase behavior and can be promising agents in several uses such as, bioplastics, drug carriers, etc.

Keywords: *Cellulose, Cellulose derivatives, Blocked isocyanate precursor, Acrylic compounds, Grafting to method, Biodegradation study.*

1. Introduction

Renewable resources are of increasing interest in our modern society, due to their positive effects on agriculture, environment and economy. Being renewable raw materials, biopolymers are gaining considerable importance, given the limited quantity of existing fossil supplies and pushed to install recent environment conservation regulations. In this context, biomass acquires enormous significance as chemical feedstock, since it consists of cellulose, hemicelluloses and lignin, etc. containing many functional groups suitable for chemical modification [1]. The cellulose and its derivatives are considered as a source of raw materials for environmentally friendly and biocompatible products [2]. They have been widely used in various industrial fields such as fibers, paper, textiles and food industry [3] and as an additive in the strengthening of bio-composites [4,5]. Cellulosic materials are generally strong, hydrophilic, and insoluble in water, stable to chemicals, safe to living bodies, reproducible, recyclable and biodegradable. In addition to these specific and advantageous characteristics, the modification techniques reinforcing their original properties or adding new functionalities have been investigated and have contributed to the development of cellulose science and technologies [6]. Furthermore, cellulose is a homopolysaccharide that is formed from linearly connecting D-glucose units condensed through the β(1−4) glycosidic bonds [7]. This polymer contains three reactive hydroxyl groups at the C-2, C-3, and C-6 atoms, which are, in general, accessible to the typical conversions of primary and secondary alcoholic OH groups [8]. The preparation of cellulose acetate (CA) is a very well known method and has been carried out at an industrial level for more than a hundred years, and is one of the many commercially important cellulose derivatives. The acetylating reaction is given in terms of the degree of substitution (DS) [9]. It's worth known that the properties of cellulose derivatives, hence their applications, depend, inter alia, on the nature of functional groups introduced, the DS, and the average degree of polymerization (DP), etc. [6]. The CA find extensive and several application domains such: automotive coatings, pharmaceuticals, cosmetics, plastics, films, textile, cigarette tow and other markets. The increasing demand for sustainable materials requires innovative ideas, flexible chemistry and more effective and more powerful process [10, 11]. As a multifunctional biological substance with a high molecular weight, and in order to improve processing ability, cellulose was used as precursor to provide different varieties of cellulose derivatives [12]. The chemical modification of cellulose is performed on the reactive hydroxyl groups on which different reactions can be carried on, and lead to prepare a broad variety of new commercial materials [13, 14]. Among of these chemical modifications which has attracted great interest, we find grafting methods [14], [15][14], [15]which have been employed as an important technique for modifying physical and chemical properties of polymers by imparting the desired and targeted properties of a polymer [15-17]. Grafting can be performed by several different methods, either by ''grafting from'', ''grafting to'' or ''grafting through'' [17]. The graft copolymerization of monomers onto cellulosic fibers has been carried out by different techniques [18], such as reversible addition fragmentation chain transfer (RAFT) polymerization [19], atom transfer radical polymerization (ATRP), reversible deactivation radical polymerization (RDRP) [20–28], and also ring-opening polymerization (ROP) [29]. Graft polymerization proceeds by these mechanisms depend on the nature of the active sites on the backbone and the monomer type [30]. Different grafted lignocellulosic natural fibers including cellulosic fibers have been reported in literature to improve elasticity, water adsorption, ion exchange capability and heat resistance of these materials using methacrylic and acrylic monomers [31, 32]. Poly(hydroxyethyl methacrylate) [33], acrylic acid [1], [34– 37], poly(acrylic Acid) [38– 41], butyl acrylate [42], glycidyl methacrylate [43], methyl methacrylate [30], [44], poly(methyl methacrylate) [10], poly(methacrylic acid) [45] and methacrylic acid and others vinyl monomers [46–49] have been attached to cellulose backbone using the techniques already cited. This modification or grafting gives new materials for composite membranes [40], metal ion sorption [36], [43], [50] and enzyme immobilization [51]. This research work is directed towards the use of chemical methods to convert renewable raw materials to valuable

industrial products. The main purpose of this work is to achieve: (a) preparation of novel derivatives through grafting of acrylic compounds with well-defined structures onto cellulose and cellulose acetate (CA) using thiol-ene reaction and addition reactions, in our knowledge, the grafting of acrylic derivatives on cellulose chains using isocyanate as a connecting agent has not been described. (b) Studying the major factors affecting the preparation of these cellulose derivatives and evaluating their properties, depending on the graft density and side chain length. (c) Characterizing the molecular structure, using FTIR and NMR spectroscopy techniques. Investigating the effect of solvents with different polarity on the solubility behavior and the biodegradation process of the derivatives prepared.

2. Experimental part

2.1. *Materials*

Cellulose was extracted from Esparto "*Stipa-tenacissima*" of Eastern Morocco, following procedures developed by *El Idrissi et al.*[52]. It was dried in a vacuum oven at 90 °C for 48 h before uses. Dibutyltindilaurate (DBTDL 95%) and 2, 2′-Azobisisobutyronitrile (AIBN) were obtained from Aldrich and used as catalysts and initiator respectively. Lithium chloride (LiCl 98%) was obtained from Riedsl-de Haëncompany. N,N-dimethylacetamide (DMAc), 1,6-hexamethylene diisocyanate (HDI 98%), 1-dodecanethiol (≥98%) (RSH), 2-hydroxyethyl methacrylate (HEMA) and 2-methacrylic acid (MAA) were purchased from Sigma-Aldrich, and all other chemicals were of analytical grade and were purchased from Sigma-Aldrich too.

2.2. *Measurements*

FTIR experiments were performed using *Shimadzu* Fourier Transform Infrared spectrometer *FTIR- 8400S* using a KBr discs containing 2% of samples and finely ground. Twenty scans were taken for each sample recorded from 4000 to 400 cm^{-1}. The FTIR spectra were accumulated at a resolution of 4 cm^{-1}. The ^{1}H NMR and ^{13}C NMR spectra were recorded on an AVANCE Bruker 300 MHz spectrometer at 360 K in Technical Scientific Research National Centre (CRNST) at Rabat Morocco. The deuterated dimethylsulfoxide (DMSO-d_6) was used as solvent and all of the spectra were recorded for 16 scans with a pulse delay of 20s. We have used the ^{1}H NMR technique to estimate the degree of substitution (DS) of CA, Cell-RSH, Cell-R'SH, CA-RSH and CA-R'SH using the equations 1 [53] and the results are summarized in table 2:

$$DS = \frac{n_{AUG} * I_i}{n_i * I_{AUG}} \qquad (1)$$

Where:

- I_i: Integration of the grafted group (i); I_{AUG}: Integration of the cellulose skeleton; and n_{AUG} and n_i: Number of protons in cellulose or CA ($n_{AUG} = 7$) and in corresponding grafted group, respectively.

$$DS_{Cell-RSH} = \frac{7I_{CH3}}{3I_{AUG(C)}} = \frac{7 * 1}{3 * 1.65} = 1.4$$

$$DS_{Cell-R'SH} = \frac{7I_{CH3}}{3I_{AUG(C)}} = \frac{7 * 1}{3 * 1.38} = 1.69$$

$$DS_{CA} = \frac{7I_{CH3}}{3I_{AUG(CA)}} = \frac{7 * 34.53}{3 * 47.63} \approx 1.7$$

$$DS_{CA-RSH} = \frac{7I_{CH3}}{3I_{AUG(CA)}} * DS_{CA} = \frac{7 * 1}{3 * 3.22} * 1.7 = 1.2$$

The global DS of the derivative CA-RSH is equal at: 1.7+1.2≈ 2.9

$$DS_{CA-R'SH} = \frac{7I_{CH3}}{3I_{AUG(CA)}} * DS_{CA} = \frac{7*1}{3*3.72} * 1.7 = 1.06$$

The global DS of the derivative CA-R'SH is equal at: 1.7+1.06 ≈ 2.7. Thermal behaviors was determined using a Thermogravimetric Analyzer TGA, Q500 from TA instruments, at heating rate of 20°C min^{-1} under a 50 mL min^{-1} nitrogen flow in the range of 25 to 600°C. The X-ray diffraction (XRD) was performed using a diffractometer system (Shimdza XRD 6000) with Cu (λ = 0.154 Å). To estimate the state order in the Cell-RSH, Cell-RS'H, CA-RSH and CA-RS'H, the crystallinity index (CrI) was calculated using the equation: 2 cited in the literature [42]:

$$CrI\ (\%) = \frac{I_{002} - I_{am}}{I_{002}} * 100 \qquad \textbf{(2)}$$

Where I_{002} is the maximum intensity (in arbitrary units) of the 002 lattice diffraction and I_{am} is the intensity of diffraction in the same units at 2θ = 18°.

3.3.Solubility study tests

Some dissolution tests of cellulose derivatives and cellulose acetate derivatives were carried out. The test is described by the following procedure. In the first step, powder samples were placed in a small weighting bottle and dried in vacuum oven at 70°C. In the second step, the dried samples were then placed in a bottle with an adequate solvent at room temperature or at 120°C for all samples, keeping the mixture under stirring until the powder disappeared (visual monitoring) and a transparent solutions are obtained.

2.4. Biodegradation tests

2.4.1. Biodegradation under solid conditions

The biodegradation under aerobic solid conditions has been standardised and adopted basically in the same form by the American Society for Testing and Materials (ASTM G21-70, G22-76, G29-75), by the French Association for normalization (AFNOR X 41-514-81 and X41-517-69), by the German Institute of Standardization (DIN 53739) and by the International Organization for Standardization (ISO 846) [54]. The tested samples were placed on the surface of a mineral salt agar (M_S) which is composed of monopotassium phosphate (KH_2PO_4: 0.7 g), potassium hydrogen phosphate (K_2HPO_4: 0.7 g), magnesium sulfate heptahydrate ($MgSO_4/7H_2O$: 0.7 g), ammonium nitrate (NH_4NO_3: 1 g), sodium chloride (NaCl: 0.005 g), ferrous sulfate heptahydrate ($FeSO_4/7H_2O$: 0.002 g), zinc sulfate heptahydrate ($ZnSO_4/7H_2O$: 0.002 g) and manganese sulfate heptahydrate ($MnSO_4/7H_2O$: 0.001 g) and agar (15 g), dissolved in sufficient distilled water to make up 1000 ml (pH ≈ 6 to 6.5). The culture medium was autoclaved at 121°C for 20 min, and then pours plated in sterile petri dishes. The test material and the agar medium are sprayed with a standardized mixed inoculum of lixivia. Petri dishes are incubated at a constant temperature for 21 to 28 days at 25°C. The test material is then subjected to the visual assessment.

2.4.2. Biodegradation tests in liquid medium

The assessment of biodegradability has been performed following the standard test method ISO 14851 [55]. Glass flasks with a 600 mL capacity were used as test vessels. The flasks were filled till a final 400 mL volume and kept closed with glass caps. The test liquid medium was the ''standard test medium'' described in the ISO 14851 (determination of the ultimate aerobic biodegradability of plastic materials in an aqueous medium-method by measuring the oxygen demand in a closed respirometer), based on the following solutions.

- Solution A: KH_2PO_4 (8.5 g/L), K_2HPO_4 (21.75 g/L), $Na_2HPO_4.2H_2O$ (33.4 g/L), NH_4Cl (0.5 g/L);
- Solution B: $MgSO_4.7H_2O$ (22.5 g/L);

- Solution C: $CaCl_2.2H_2O$ (36.4 g/L);
- Solution D: $FeCl_3.6H_2O$ (0.25 g/L).

The test medium was prepared by adding solution A (10 mL), solutions B, C, and D (1 mL each) to about 500 mL of water and bringing the volume to 1000 mL with water. The inoculum solution was prepared as follows. A sample was drawn from the soil, diluted with water in order to reach final total solids concentration of 200 g/L, and aerated for 4 h. Each vessel was filled with 380 mL of test medium and inoculated with 20 mL of inoculums solution. Test or reference material was added to each vessel (50 mg), with the exception of the blanks. Two replicates were used for each material and for blanks. The tests were stopped when O_2 consumption was no longer detectable, in all cases at least after three months. The Oxitop system used in the determination of BOD contains an individual number of reactors consisting of glass bottles with a carbon dioxide trap (sodium hydroxide) in the headspace. The bottles are supplied with a magnetic stirrer and sealed with a cap containing an electronic pressure indicator. Afterwards, each vessel was kept under aeration for 15 min to restore the original oxygen concentration of the liquid medium. The vessels were then closed and put back in incubation. The net biochemical oxygen demand (BOD) of the test material was calculated as the difference between oxygen consumption in the test and in the blank flasks using the equation (3):

$$net\ BOD = BOD_{tm} - BOD_b \quad \textbf{(3)}$$

Where: BOD_{tm} is the total biochemical oxygen demand of the test material from one flask; BOD_b is the biochemical oxygen demand of the blanks (average of two flasks).

The percentage of biodegradation D_{tm} is calculated as the ratio of the net biochemical oxygen demand to the total theoretical oxygen demand (total ThOD, referred to the amount of test material introduced originally in the flask) using the equation (4):

$$D_{tm} = \frac{net\ BOD}{total\ ThOD} \times 100 \quad \textbf{(4)}$$

with: D_{tm}: Percentage of biodegradation; net BOD: Specific Biochemical Oxygen Demand (in mg O_2/L); and ThOD: Theoretical Oxygen Demand (in mg O_2/L). and The ThOD of the polymer $n(C_cH_hO_oN_nS_s)$, with a relative molecular mass Mr (per monomer), was calculated according to:

$$ThOD = \frac{31.9988(c+0.25(h-3n)+1.5S-0.5o)}{M_r} \quad \textbf{(5)}$$

2.5. Synthetic procedures

2.5.1. Extraction of cellulose and preparation of cellulose acetate (CA)

Firstly, the cellulose used in this work was extracted in an alkaline medium and its degree of polymerization (DP) was estimated from the intrinsic viscosity value using Mark-Houwink equation ($DP_w \approx 1402$ and $M_w \approx 227200$ g/mol) [52]. Secondly, the cellulose solution was obtained by dissolving cellulose in a mixture of DMAc/LiCl following the method reported in the literature by Araki et al. [56]. Furthermore, the CA was prepared according to the method described in the literature by Doyle and Pethrick [57] and its DS was obtained using NMR method.

2.5.2. Preparation of the Cell-RSH and Cell-R'SH

A blocked isocyanate compounds (precursors) were prepared using the following steps. First, in a three-necked round-bottom flask equipped with an addition funnel, thermometer, magnetic stirrer and a reflux condenser, 1.25 mmol of acrylic function (HEMA (R) or MAA(R')) were introduced. 1.25 mmol of 1-dodecanethiol and $1.25 * 10^{-2}$ of AIBN were placed in the funnel and was added dropwise to the reaction mixture. The system was kept under stirring in nitrogen atmosphere at 80°C for 3 h; telomeres having the following structures $CH_3(CH_2)_{11}$-S-$(CH_2$-$CCH_2COOR")_n$-H ,where R": H or -$(CH_2)_2OH$ were obtained (figure 1a). During this thiol-ene additions monoadducts were mostly

formed with high yield. Secondly, in another three-necked round-bottom flask equipped with an addition funnel, thermometer, magnetic stirrer and a reflux condenser, 2.5 mmol of 1,6-hexamethylene diisocyanate was introduced. The monoadducts already prepared in the first step with a relative amount of DBTDL were singly placed in the funnel and were added dropwise to 1,6-hexamethylene already placed in the round-bottom. The mixture is maintained at 80°C for 3 h and kept under stirring under nitrogen atmosphere, and then, the blocked isocyanate is formed with a high yield (figure 1b). Finally, the cellulose solution already prepared (2.5 mmol) was added dropwise to the mixture contained the blocked isocyanate; this addition reaction is catalyzed by DBTDL and the mixture was kept under stirring at 80°C for 3 h in nitrogen atmosphere. The final product (grafted cellulose) was isolated after precipitation in a mixture of methanol/water (1/3), filtrated using a membrane filter and washed with distilled water, methanol and dried under vacuum at 80°C. All these reactions were followed by FTIR technique. The obtained derivatives were characterized by their ^{1}H-NMR and ^{13}C-NMR spectra. The NMR data are given below.

Cell-RSH; ^{1} H-NMR (300 MHz, DMSO, 25°C, ppm): δ 0.83 ($\underline{CH_3}$-$(CH_2)_{11}$S-)); 1.10 - 1.58 (-$\underline{(CH_2)_{10}}$-CH_2-S-, -CO-HC($\underline{CH_3}$)-CH_2-S- and -NH-CH_2-$\underline{(CH_2)_4}$-CH_2-NH-); 2.48 (-S-$\underline{CH_2}$-); 2.73 (-CO-$\underline{HC}$(CH_3)-CH_2-S-); 2.85 – 3.09 (-CO-HC(CH_3)-$\underline{CH_2}$-S- and -NH-$\underline{CH_2}$-$(CH_2)_4$-$\underline{CH_2}$-NH-); 4.12 (-O-$\underline{CH_2}$-$\underline{CH_2}$-O-); 3.37 - 4.81 (CH of AUG_{Cell}); 4.12 (CH_2 of AUG_{Cell}) and 7.14 (NH). ^{13} C-NMR (300 MHz, DMSO, 25°C, ppm) δ: 14.39 ($\underline{CH_3}$-$(CH_2)_{11}$S-); 16.85 (-CO-HC($\underline{CH_3}$)-CH_2-S-); 22.18 - 32.26 (-$\underline{(CH_2)_{10}}$-CH_2-S- and -NH-CH_2-$\underline{(CH_2)_4}$-CH_2-NH-); 34.15 (-S-$\underline{CH_2}$-); 35.01 (-CO-HC(CH_3)-$\underline{CH_2}$-S-); 40.47 (-NH-$\underline{CH_2}$-$(CH_2)_4$-$\underline{CH_2}$-NH- and -CO-$\underline{HC}$(CH_3)-CH_2-S-); 62.02 (-NH-CO-O-$\underline{CH_2}$-CH_2-O-CO-HC(CH_3)); 62.80 (-O-CH_2-$\underline{CH_2}$-O-); 63.19 (CH_2 of AUG_{Cell}); 69.9 -75.3 (CH of AUG_{Cell}); 158.7 (-$\underline{CO}$-NH-(CH2)-NH-$\underline{CO}$-) and 165.9 (-$\underline{CO}$-HC(CH_3)-).

Cell-R'SH; ^{1} H-NMR (300 MHz, DMSO, 25°C, ppm) δ: 0.83 ($\underline{CH_3}$-$(CH_2)_{11}$S-)); 1.10 - 1.60 (-$\underline{(CH_2)_{10}}$-CH_2-S- and -NH-CH_2-$\underline{(CH_2)_4}$-CH_2-NH-); 2.49 (-S-$\underline{CH_2}$-); 2.71 (-CO-$\underline{HC}$(CH_3)-CH_2-S-); 2.88 – 3.12 (-CO-HC(CH_3)-$\underline{CH_2}$-S- and -NH-$\underline{CH_2}$-$(CH_2)_4$-$\underline{CH_2}$-NH-); 3.14 - 4.52 (CH of AUG_{Cell}); 3.6 (CH_2 of AUG_{Cell}); 7.10 (NH). ^{13} C-NMR (300 MHz, DMSO, 25°C, ppm) δ: 14.40 ($\underline{CH_3}$-$(CH_2)_{11}$S-); 16.60 (-CO-HC($\underline{CH_3}$)-CH_2-S-); 22.22 – 32.68 (-$\underline{(CH_2)_{10}}$-CH_2-S- and -NH-CH_2-$\underline{(CH_2)_4}$-CH_2-NH-); 32.02 (-$\underline{CH_2}$-S-$\underline{CH_2}$-); 34.48 (-CO-HC(CH_3)-$\underline{CH_2}$-S-); 40.46 (-NH-$\underline{CH_2}$-$(CH_2)_4$-$\underline{CH_2}$-NH-); 40.75 (-CO-$\underline{HC}$(CH_3)-CH_2-); 70.61 -75.11 (CH of AUG_{Cell}); 62.03 (CH_2 of AUG_{Cell}); 159.3 (-O-$\underline{CO}$-NH-); 175.30 (-NH-$\underline{CO}$-HC(CH_3)-).

2.5.3. Preparation of the grafted cellulose acetate CA-RSH and CA-R'SH

As it has already been done for the cellulose, 2.5 mmol of blocked isocyanate (precursor) was introduced into a three-necked round-bottom flask equipped with an addition funnel, thermometer, magnetic stirrer and a reflux condenser. The system was kept under nitrogen atmosphere at 80°C for 3 h and under stirring. The CA (DS = 1.7) solubilised in DMSO with relative amount of DBTDL was added slowly to the solution in the flask. The grafted CA compounds (CA-RSH or CA-R'SH) are isolated after a precipitation in methanol, filtration and successively washing with distilled water and methanol, and finally dried in an oven at 60°C for 24 h. All derivatives were characterized by their ^{1} H-NMR and ^{13} C-NMR spectra. The NMR data are also listed below.

CA-RSH; ^{1} H-NMR (300 MHz, DMSO, 25°C, ppm) δ: 0.83 ($\underline{CH_3}$-$(CH_2)_{11}$S-)); 1.00 - 2.10 (-$\underline{(CH_2)_{10}}$-CH_2-S-, -CO-HC($\underline{CH_3}$)-CH_2-S- and -NH-CH_2-$\underline{(CH_2)_4}$-CH_2-NH-); 2.48(-S-$\underline{CH_2}$-); 2.72 (-CO-$\underline{HC}$(CH_3)-CH_2-S-); 2.85 - 3.08 (-CO-HC(CH_3)-$\underline{CH_2}$-S- and -NH-$\underline{CH_2}$-$(CH_2)_4$-$\underline{CH_2}$-NH-); 4.51 (-O-$\underline{CH_2}$-$\underline{CH_2}$-O-); 3.25 - 4.85 (CH of AUG_{CA}); 4.11 (CH_2 of AUG_{CA}); 2.15 (CH_3 of AUG_{CA}); 7.13 (NH). ^{13} C-NMR (300 MHz, DMSO, 25°C, ppm) δ: 14.39 ($\underline{CH_3}$-$(CH_2)_{11}$S-); 16.84 (-CO-HC($\underline{CH_3}$)-CH_2-S-); 22.55 - 31.75 (-$\underline{(CH_2)_{10}}$-CH_2-S- and -NH-CH_2-$\underline{(CH_2)_4}$-CH_2-NH-); 32.03 (-S-$\underline{CH_2}$-); 34.12 (-CO-HC(CH_3)-$\underline{CH_2}$-S-); 39.08 - 39.64 (-NH-$\underline{CH_2}$-$(CH_2)_4$-$\underline{CH_2}$-NH- and -CO-$\underline{HC}$(CH_3)-CH_2-S-); 61.15 (-NH-

CO-O-$\underline{CH_2}$-CH_2-O-CO-HC(CH_3)); 62.04 (-O-CH_2-$\underline{CH_2}$-O-CO-HC(CH_3)); 71.83 - 84.76 (CH of AUG_{CA}); 63.16 (CH_2 of AUG_{CA}); 21.02 (CH_3 of AUG_{CA}); 158.29 (-$\underline{CO}$-NH-(CH2)-NH-$\underline{CO}$-); 170.80 (-$\underline{CO}$-HC(CH_3)-).

CA-R'SH; ^{1} H-NMR (300 MHz, DMSO, 25°C, ppm) δ: 0.83 ($\underline{CH_3}(CH_2)_{11}$S-)); 1.12 - 2.10 (-$\underline{(CH_2)_{10}}$-$CH_2$-S-, -OC-HC($\underline{CH_3}$)-$CH_2$-S- and -NH-$CH_2$-$\underline{(CH_2)_4}$-$CH_2$-NH-); 2.48 (-S-$\underline{CH_2}$-); 2.73 (-CO-$\underline{CH}$($CH_3$)-$CH_2$-S-); 2.87 - 3.10 (-CO-CH(CH_3)-$\underline{CH_2}$-S- and -NH-$\underline{CH_2}$-$(CH_2)_4$-$\underline{CH_2}$-NH-); 3.40 - 4.80 (CH of AUG_{CA}); 4.21 (CH_2 of AUG_{CA}); 2.16 (CH_3 of AUG_{CA}); 7.28 (NH). ^{13} C-NMR (300 MHz, DMSO, 25°C, ppm) δ: 14.41 ($\underline{CH_3}$-$(CH_2)_{11}$S-); 16.79 (-CO-HC($\underline{CH_3}$)-CH_2-S-); 24.44 - 30.98 (-$\underline{(CH_2)_{10}}$-CH_2-S- and -NH-CH_2-$\underline{(CH_2)_4}$-CH_2-NH-); 32.50 (-$\underline{CH_2}$-S-CH_2-); 34.73 (-CO-HC(CH_3)-$\underline{CH_2}$-S-); 39.64 and 40.20 (-NH-$\underline{CH_2}$-$(CH_2)_4$-$\underline{CH_2}$-NH-); 40.76 (-CO-$\underline{HC}$(CH_3)-CH_2-); 70.20 - 84.04 (CH of AUG_{CA}); 62.31 (CH_2 of AUG_{CA}); 21.03 (CH_3 of AUG_{CA}); 159.39 (-O-$\underline{CO}$-NH-); 170.86 (-NH-$\underline{CO}$-HC(CH_3)-).

3. Results and discussion

3.1. Synthesis

The modification of cellulose and CA was conducted using grafting onto method using acrylic compounds (HEMA, MAA), R-SH and 1, 6-HDI. This grafting process was conducted in three steps, firstly, the graft chain was lengthened by a reaction between 1-dodecanethiol (R-SH) and acrylic compounds (HEMA (R), MAA (R')) (figure 1a) using telomerization technique. It has been monitored that in this thiol-ene addition, the acrylic function is considered as taxogen, R-SH as telogen and AIBN as initiator and the products obtained are named telomeres [58]. The thiol-ene addition was conducted in free-solvent and under conditions allowing to reach mostly the monoadduct and the reaction advancement was followed by FTIR technique. The absorbance band of the SH and -C=C- groups assigned at 2574 cm^{-1} and 1638 cm^{-1} respectively despaired justifying that the addition reaction is established. In the second step, a blocked isocyanate compound is prepared by reacting one of the functional groups of the (1, 6)-HDI with the end group (-OH or -COOH) of the monoadducts already prepared using DBTL as catalyst (figure1b). The FTIR spectra of these precursor show a new sharp peak around 2270 cm^{-1} assigned to the presence of NCO group situated at the end. Then, at the last step; cellulose and CA respectively were reacted with blocked isocyanate compounds already described following grafted onto method (figure 1c).

(a)

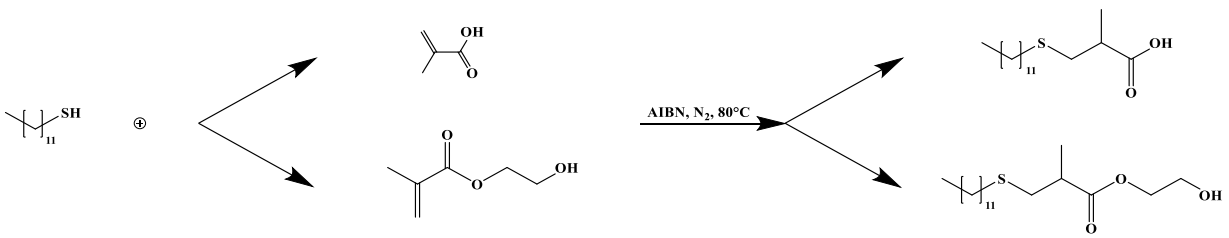

Figure 1a: Preparation of: (a) the monoadducts

(b)

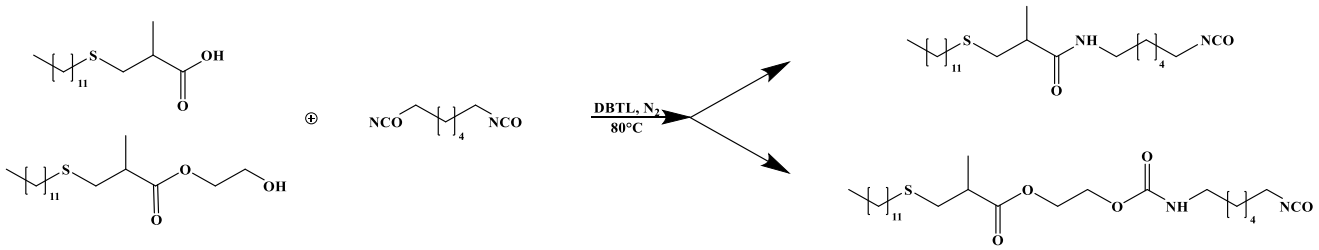

Figure 1b: Preparation of: (a) the blocked isocyanate (precursors)

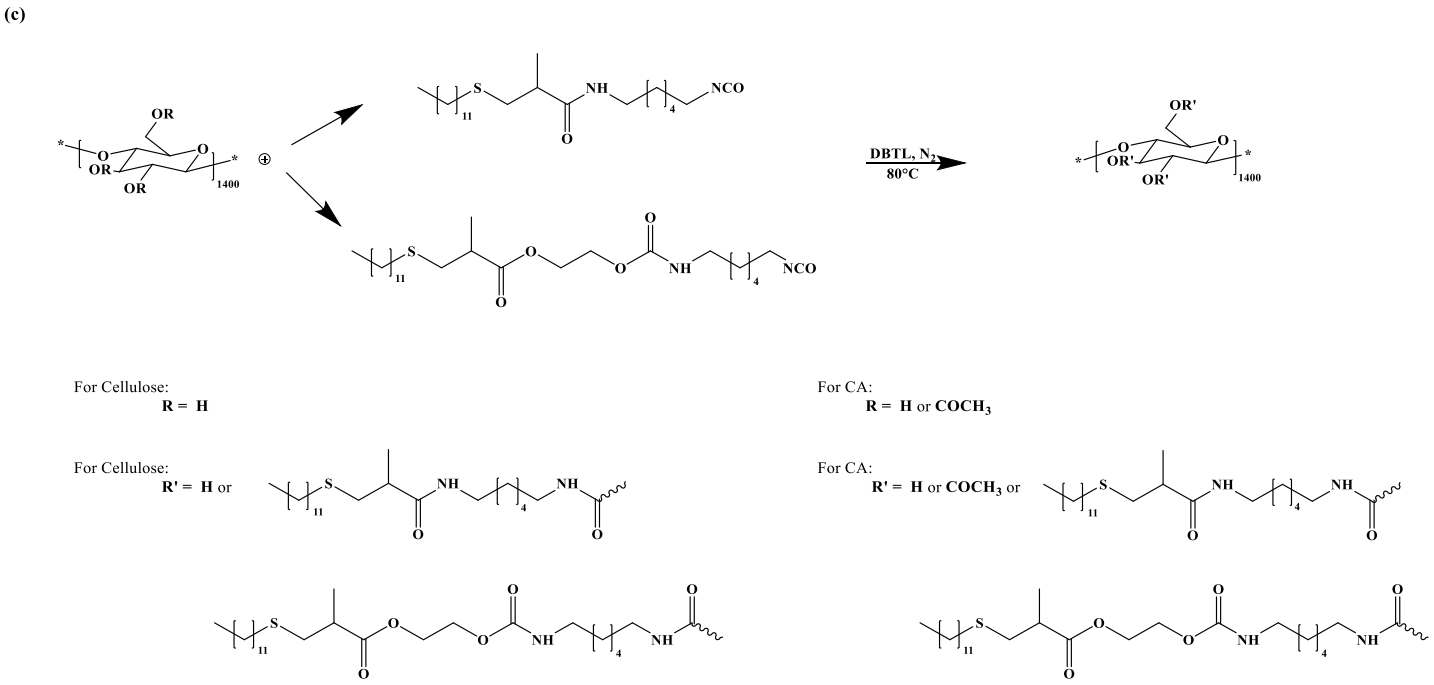

***Figure** 1c:* Preparation of: (c) the grafted cellulose and CA

This method, in our opinion, has certain advantages compared to other methods such as grafting from and grafting through, especially when the isocyanate groups are used as coupling agent. Firstly, using this method high DS and the length of the grafted chains can be controlled and reached easily. Furthermore, this method also does not generate residues and toxic products during the grafting process contrary to other methods already mentioned. Also, the formation of homopolymers is absent contrary to ATRP, RAFT and ROP procedures.

3.2. NMR analysis

^{1}H NMR spectroscopy was used to characterize the cellulose and its derivatives prepared here (Cell-RSH and Cell-R'SH). Examples of ^{1}H NMR spectra of these products are shown in Fig. 2. Grafting to the cellulose backbone was confirmed by several characteristic signals. The protons of aliphatic chains appeared from 0.83 to 4.12 ppm (fig. 2a). The cellulosic backbone shows some peaks from 3.37 to 4.81 ppm for Cell-RSH (carbohydrate protons). These results are in argument with those cited in the literature [11]. Moreover, the protons of the methylene groups of the cellulose backbone (-CH_2-) give a signal at 4.12 ppm for Cell-RSH. The characteristic peaks at 7.14 ppm are attributed to the peaks of the urethane group (-NHCO-O-). The ^{1}H NMR spectra of the CA-RSH are presented in figure 2b. In the case of CA-RSH (figure 2b), the presence of some signals situated between 0.83 ppm and 4.51 ppm indicates that the modification of CA by aliphatic chain was established. The peak of the urethane group (-NHCO-O-) appears at 7.13 ppm. The signals of CA backbone appear between 3.25 and 4.85 ppm, and the acetyl group protons appear at 2.15 ppm. The signals in the ^{13}C NMR spectra of the products Cell-RSH and CA-RSH, situated between 14.39 ppm and 62.80 ppm, and between 14.39 ppm and 62.04 ppm (figure 3a and 3b), are typically attributed to the -CH_2- of aliphatic carbons and constitute the first indication that the precursor (RSH-HDI) are attached to the cellulose and CA chains. These results are in agreement with those cited in the literature [11]. The signals of the cellulose backbone appeared in the range 69.9 - 75.3 ppm for Cell-RSH. A peak situated at 63.19 ppm is attributed to the protons of the methylene group (-CH_2-) of cellulose backbone in Cell-RSH. Furthermore, the signals characterizing urethane carbonyl group in the case of Cell-RSH appear at 158.7 ppm and a signal characterizing ester carbonyl groups give a signals at 165.9

ppm [59]. The signals of the carbons of the CA backbone appear from 71.83 to 84.76 ppm for CA-RSH and the signals characterizing the carbonyl groups are around 158.29 and 170.80 ppm corresponding, respectively, to the urethane carbonyl and the ester carbonyl groups (CA-RSH).

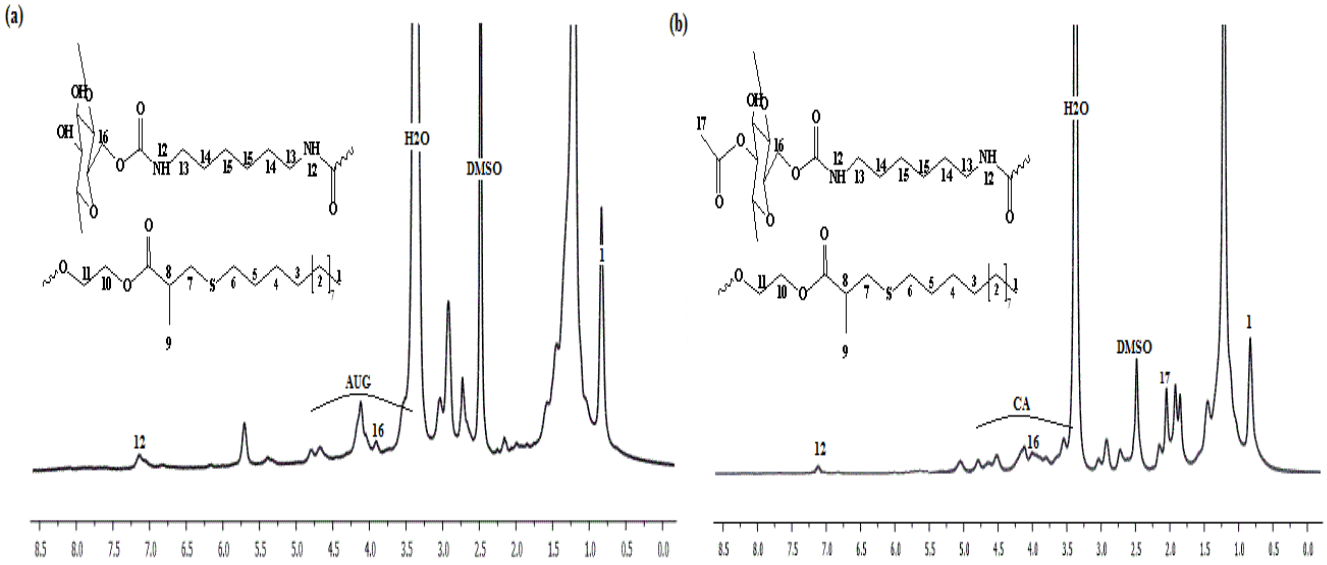

Figure 2: An example of [1]H, NMR spectra of (a) Cell-HDI-RSH and (b) CA-HDI-RSH

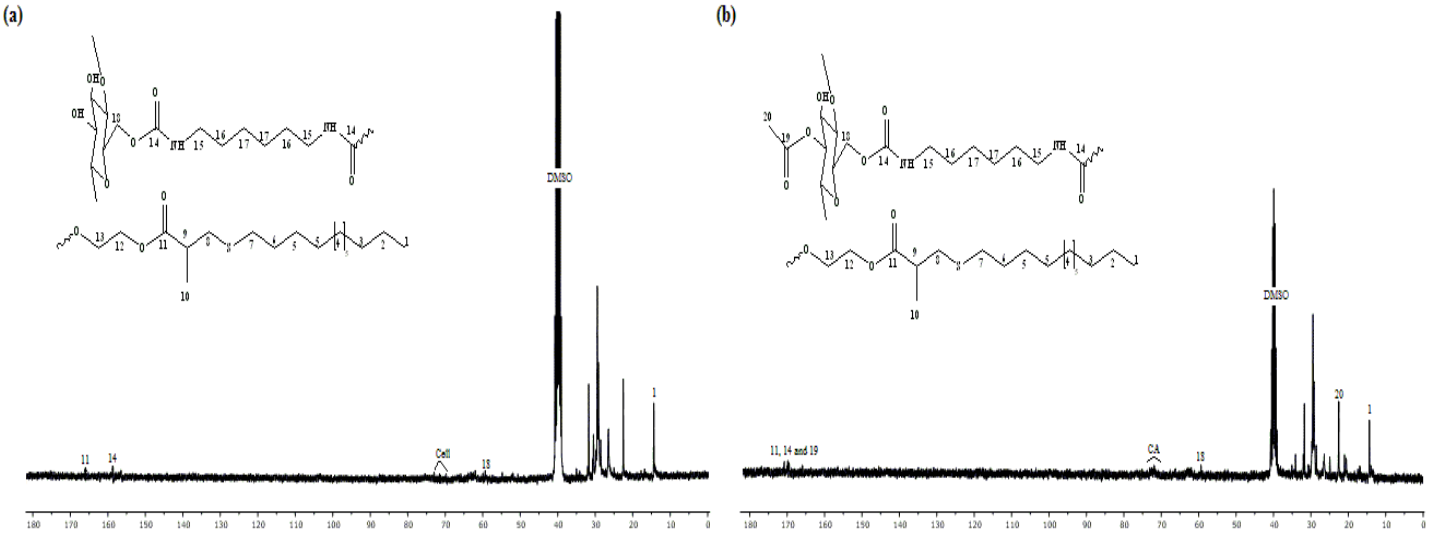

Figure 3: An example of ^{13}C NMR of (a) Cell-RSH and (b) CA-RSH

3.3. Characterization by FTIR analysis

The derivatives obtained were characterized by their FTIR. Fig. 4 shows the FTIR spectra of cellulose, Cell-RSH, Cell-R'SH, CA, CA-RSH and CA-R'SH. In the spectrum of cellulose (Fig. 4a), strong bands at 3396 cm^{-1} and 1058 cm^{-1} are attributed respectively to -OH stretching and C-O-C in anhydroglucose units. In comparison, the spectrum of CA shows the presence of three important adsorption bands assigned to the functional vibrations at 1751 cm^{-1} ($\upsilon_{C=O}$), 1375 cm^{-1} (υ_{-CH3}), and 1236 cm^{-1} (υ_{C-O})). In addition, a reduction in the intensity of the hydroxyl groups (-OH) at 3431 cm^{-1} due to acetylating reaction was noted. The band situated at 2899 cm^{-1} is associated to stretching vibration of -CH- and the absorption band at 1647 cm^{-1} corresponds to naturally absorbed water [60]. Furthermore, the absorption band at 895 cm^{-1} is a characteristic of the β-glucidic bond. Fig. 4a also, gives the FTIR spectra of cellulose derivatives

(Cell-RSH and Cell-R'SH), it can be seen that comparing with the spectrum of cellulose, the apparition of some novel absorption bands around 1740 cm^{-1} (-NHCO-O), 1560 cm^{-1} (-NH-), 1260 cm^{-1} (C-O) and 625 cm^{-1} (C-S) indicates the success formation of these derivatives. Additionally, a decrease in the intensity of the absorption band around 3330 cm^{-1} (-OH) and the intensity of the peaks around 2855 cm^{-1} and 2927 cm^{-1} increases showing that this grafting -to-method was successful and the expected derivatives are obtained. The stretching vibration of -NH-CO-O appeared around 3300cm^{-1}.

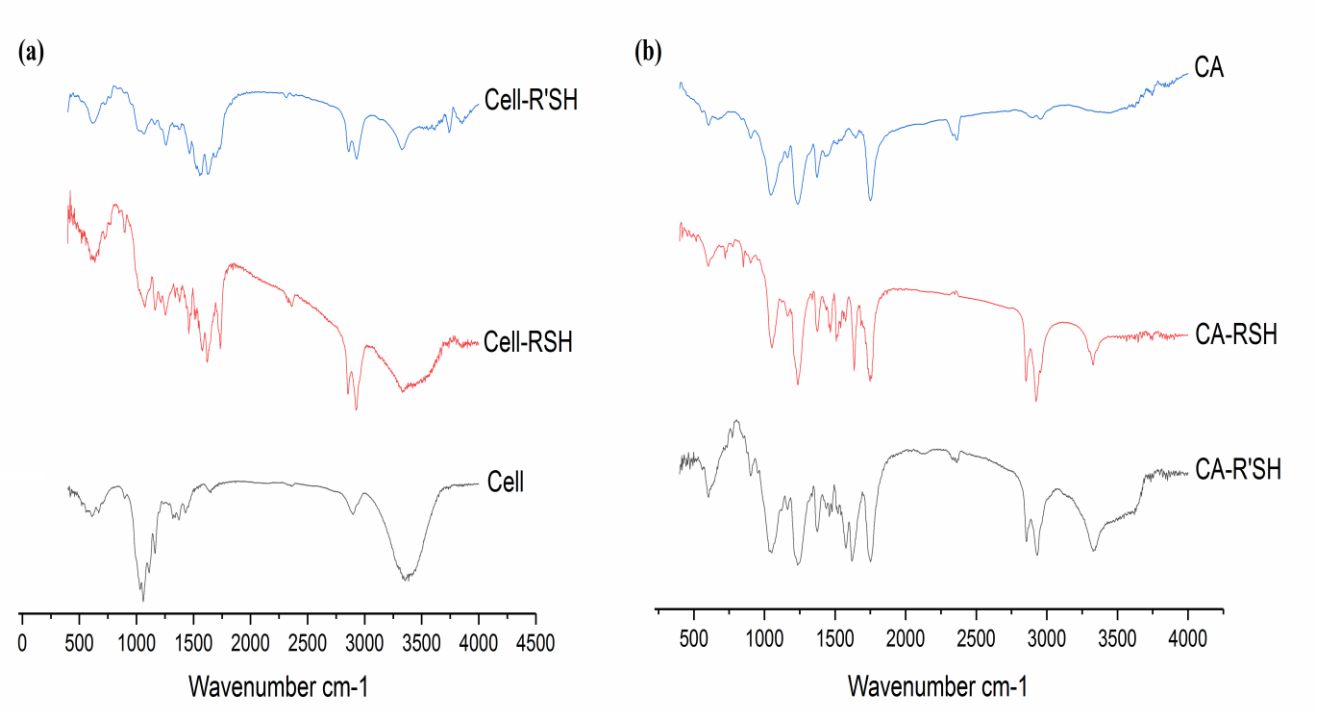

Figure 4: FTIR spectra of (a) cellulose, Cell-RSH, Cell-R'SH and (b) CA, CA-RSH and CA-R'SH

The FTIR spectra of the CA and its derivatives are presented in Fig.4b, they give an absorption band located at 1751 cm^{-1} assigned to the C=O stretching vibration of the ester group of CA ($CH_2C=O$). It's worth noticing that the FTIR spectrum of the CA shows a decrease in the absorption intensity of the band located at around 3431 cm^{-1} assigned to the stretching of the hydroxyl groups compared with the cellulose spectrum. This decreasing occurs because a part of hydroxyl groups are substituted by acetyl groups [61]. Furthermore, the FTIR spectra of CA-RSH and CA-R'SH show some new absorption bands around 1750, 1560, 600 cm^{-1}. These bands are assigned respectively to the stretching vibration of the urethane group (-NHCO-O-), the bending vibration of the N-H, and the stretching vibration of the sulfur band (C-S). The peak around 1757 cm^{-1} is assigned to the C=O stretching vibration of the ester group (CH_3CO-O-) situated in CA backbone. The decrease of the intensity of the peak around 3327 cm^{-1} (-OH) and the increase of the intensity peaks around 2850 cm^{-1} and 2925 cm^{-1} (CH/CH_2), confirm that the reaction between the remaining hydroxyl groups of CA and the isocyanate group of precursors is achieved during all these grafting onto tests. It's worth noticing that the absorption vibration of NCO group (2270 cm^{-1}) situated at the end of the precursor disappeared completely. These results are in agreement with those cited in the literature [62].

3.4. XRD analysis

XRD results show some important information about the grafted reactions and lattice of cellulose and CA compounds. The XRD patterns of the cellulose, Cell-RSH, Cell-R'SH, CA, CA-RSH and CA-R'SH are presented in Figure 5. It can be seen that cellulose (Fig.5a) has 2θ diffraction peaks at 13.82°, 16.30°, 22.04° and 34.10°; assigned to the $10\bar{1}$,

101, 002, and 040 diffraction planes respectively [63], justifying the typical cellulose I (I_α and I_β) crystalline form [62]. The XRD patterns of Cell-RSH display some new peaks around 2θ = 14.73°, 15.06°, 19.74°, 22.42° and 34.45° showing the presence of new crystal planes. In addition for Cell-RS'H, the new peaks situated at 2θ = 13.64°, 14.40°, 17.71°, 20.77°, 23.91° and 24,70° showed also the presence of new crystal planes. It can be noted that the grafting process was successful and a change occurred in the morphology of cellulose.

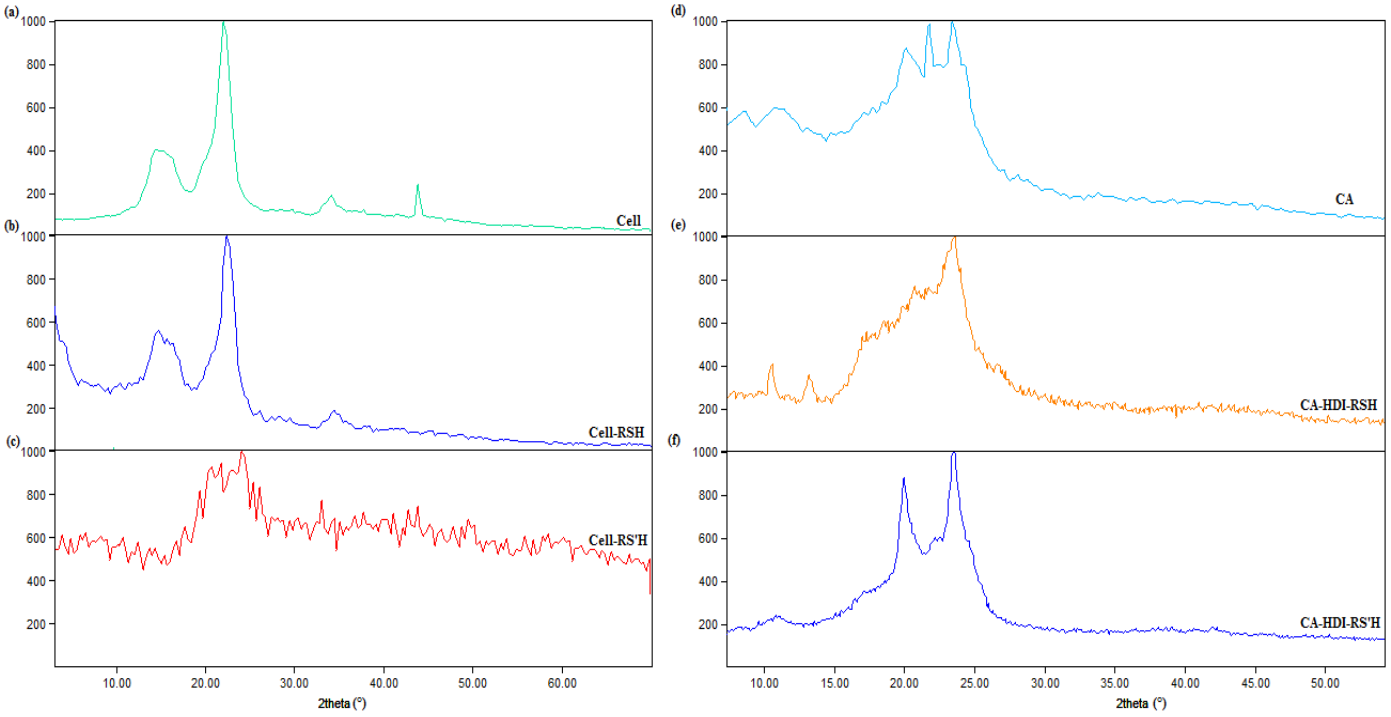

Figure 5: XRD spectra of (a) cellulose, (b) Cell-RSH, (c) Cell-RS'H (d) CA, (e) CA-RSH, and (f) CA-R'SH

XRD pattern of the CA in figure 5d shows diffuse peaks around 2θ = 8.05°, 20.75°, 24.09°, 41.47° and 49.49° with two maxima at 2θ = 17° and at 24°, showing its semi crystalline appearance. These results are in agreement with those reported in the references [61], [64]. The main peak located at approximately 8.05° was cited as the principal characteristic of the semi-crystalline acetylated derivative cellulose [61]. In modified CA, introducing acrylic compounds has an effect on CA morphology, where the major reflections are at 2θ = 10.52°, 13.23°, 16.70°, 20.69°; 23.42° and 27.31° for CA-RSH and at 2θ = 10.99°, 18.10°, 20.02°, 23.54° and 24.80° for CA-RS'H.

Table 1: Crystallinity index (CrI) of cellulose and its derivatives

Samples	Crystallinity index (CrI(%))
Cellulose	88
Cell-RSH	80
Cell-RS'H	62
CA	64
CA-RSH	54
CA-RS'H	59

The acetylated cellulose presents a low degree of crystallinity (64%) compared with that of the cellulose (88%) due to the substitution of the hydroxyl groups by acetyl groups with greater volume, which broke the inter- and intra-

molecular hydrogen bonds of cellulose [65]. The CrI decreases from 88% for cellulose to 80% for Cell-RSH and 62% for Cell-RS'H indicating that the content of the amorphous regions increases significantly, allowing their modification and transformation to occur easily [6]. This difference is probably due to the difference in the values of grafting percentages or the values of DS (1.4; 1.7). In addition, this fact indicates that the product has lost its crystallinity after the fibers modification. For CA and CA derivatives, a small variation in the crystallinity index between CA (64%), CA-RSH (54%) and CA-RS'H (59%) was observed. The X-ray diffraction studies showed that crystallinity depends greatly on the structure of the reagents and the reaction conditions. It can be concluding that degree of crystallinity depends greatly on the values of DS and the nature of the molecules grafted. It can be noted that, in the case of CA; the CrI values were not greatly influenced during this graft process; despite; the DS globally reaches values that tend towards 3.

3.5. Solubility study

The solubility phenomena is an important result characterizing the miscibility of a system under qualitative aspects [66]. Some dissolution tests of Cell-RSH, Cell-R'SH, CA-RSH and CA-R'SH were carried out. The test was described by the following procedure. In the first step, powder samples were placed in a small weighting bottle and dried in vacuum oven at 70°C. In the second step, the dried samples were then placed in a bottle with an adequate solvent at room temperature for derivatives of CA and at high temperature for other samples, keeping the mixture under stirring until the powder disappeared (visual monitoring) and a transparent solutions are obtained. According to our recent study, it is well-known that the introduction of carbamate groups on the cellulose and CA backbones leads to the increase of their solubility, especially in polar solvent systems.

Table 2: Solubility tests of grafted cellulose derivatives and they DS

		Cell-RSH (DS = 1.4)	Cell-R'SH (DS = 17)	CA-RSH (DS = 1.2)	CA-R'SH (DS = 1.1)
Polar protic solvents	Ethanol	-	-	-	-
	Methanol	-	-	-	-
	water	-	-	-	-
	Propane-2-ol	-	-	-	-
Polar aprotic solvents	DMSO	+	+	+	+
	DMAc	+	±	+	±
	DMF	±	±	±	±
	Acetone	-	-	-	-
	Acetonitrile	-	-	-	-
Non-polar aprotic solvents	Chloroform	-	-	-	-
	Dichloromethane	-	-	+	-
	Toluene	-	-	-	-
	Hexane	-	-	-	-
	Tetrahydrofuran	-	-	-	-
	Diethyl ether	-	-	-	-

+: Soluble, ±: Partly soluble, -: insoluble

Table 1 lists the solubility of the cellulose derivatives prepared: Cell-RSH, Cell-R'SH, CA-RSH and CA-R'SH, generally, all these products are soluble in DMSO. For Cell-RSH and CA-RSH, they are totally soluble in DMAc and partly in DMF. In addition, CA-RSH compound is soluble in CH_2Cl_2. It can be concluded that the solubility behavior of these compounds in solvent systems depends mainly on their chemical structure, but it is also influenced by the values of DS. In addition, Cell-R'SH and CA-R'SH are also partly soluble in DMAc and DMF. In summary, the carbamates compounds synthesized are generally soluble in polar and aprotic solvent systems. Moreover, no big differences are noted between the solubility behavior between cellulose and CA derivatives.

3.6. Degradation study

3.6.1. Thermal degradation

Thermal degradation of cellulose, CA and their derivatives was studied using thermogravimetric analysis (TGA). Fig 6 shows TGA curves in the form of weight loss. In general, the curves of Cell-RSH, Cell-R'SH, CA-RSH and CA-R'SH present a same decomposition aspect taking place in three steps. The first one, starts after elimination of the residual solvents especially residual water, this step presents the degradation of the grafted groups. The second one is a decomposition of the cellulose or CA main chains and the third one is a decomposition of the residues. Comparing the thermal degradation of the simples (Cell-RSH and Cell-R'SH) to that of cellulose, several differences can be seen. Firstly, the cellulose exhibits one step rapid mass degradation and drop to about 350°C. On the other hand, the derivatives Cell-RSH and Cell-R'SH show major degradation phenomena occurring in three stages. Which are situated between 156 and 500°C for Cell-RSH and between 110 and 480°C for Cell-R'SH. It can be noted that these both compounds present different degradation steps taking into account their weight loss percent and their degradation range of temperature.

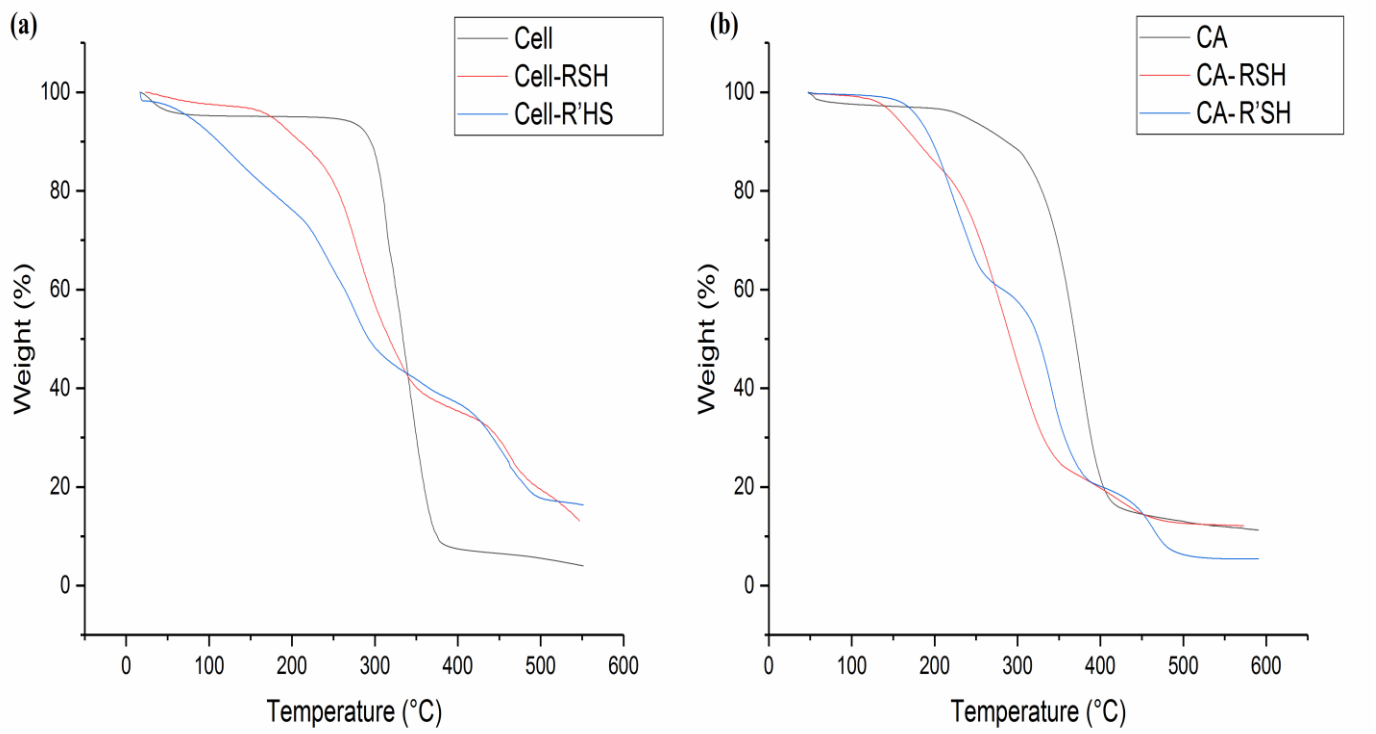

Figure 6: TGA curves of (a) cellulose, Cell-RSH and Cell-R'SH (b) and CA, CA-RSH and CA-R'SH

In the case of the CA derivatives, CA-RSH and CA-R'SH have a different degradation behaviour comparing to degradation aspect of CA, their degradation phenomena similarly to cellulose derivatives occurs in three stages. The

CA presents two degradation stages; the predominant step shows a rapid mass degradation and drop to about 320°C. The degradation steps of CA-RSH and CA-R'SH compounds takes place respectively between 100°C and 460°C for CA-RSH and between 125 and 480°C for CA-R'SH. Moreover, similarities were observed between the weight losses curves for derivatives cell-RSH and CA-RSH on the one hand and those of cell-R'SH and CA-R'SH on the other hand. All these derivatives showed a low thermal stability compared to CA and cellulose. This difference is probably due to the introduction of carbamate and acrylic groups into the cellulose and CA backbone. Moreover, the crystallinity levels and the interchains interactions in these derivatives decreased leading to a decrease of their thermal stability. iThe results indicated the thermal stability of cellulose and CA and their weight loss curves was remarkably modified by the nature and the density of grafting.

3.6.2. Biodegradation process

The International Standard ISO (ISO 846 and ISO 14851), the American Society for Testing Materials ASTM (G21-70, G22-76 and G29-75), the French Association of Normalisation (AFNOR(X 41-514-81 and X41-517-69)) and the German Deutsches Institut für Normung (DIN 53739) were adopted for determining the aerobic biodegradability under solid and liquid conditions of the blank test, the cellulose, the Cell-RSH, the Cell-R'SH, the CA, the CA-RSH and the CA-R'SH. The aerobic biodegradation experiments in solid conditions were validated by a visual assessment showing the amount of growth on the surface of the material or clear areas due to the hydrolysis of the substrate by the enzymes released by the microorganisms. The cellulose, the Cell-RSH, the Cell-R'SH, the CA, the CA-RSH and the CA-R'SH were placed on the agar medium in a Petri dish, inoculated with lixivia and incubated at 25°C for 28 days. After completing this date of incubation, it is noted visually that the cellulose, its derivatives (Cell-RSH and Cell-R'SH), CA and its derivatives (CA-RSH and CA-R'SH) were largely colonized colonized, with variable incidence, by micro-organisms, but in the absence of biopolymers (the blank test), we did not show any development of the microorganisms associated to the lixivia, composed mainly of fungi, indicating that the microorganisms used cellulose, CA and their derivatives as a source of carbon for their growth. The results are reported in figure 7. From this figure (Fig.7), it can be seen that the cellulose was colonized by bacteria more than CA and the cellulose derivatives were colonized by micro-organisms more than CA derivatives. In addition, the CA-RSH and CA-R'SH are the least colonized by microorganisms. These results will be proven by biochemical oxygen demand (BOD) tests.

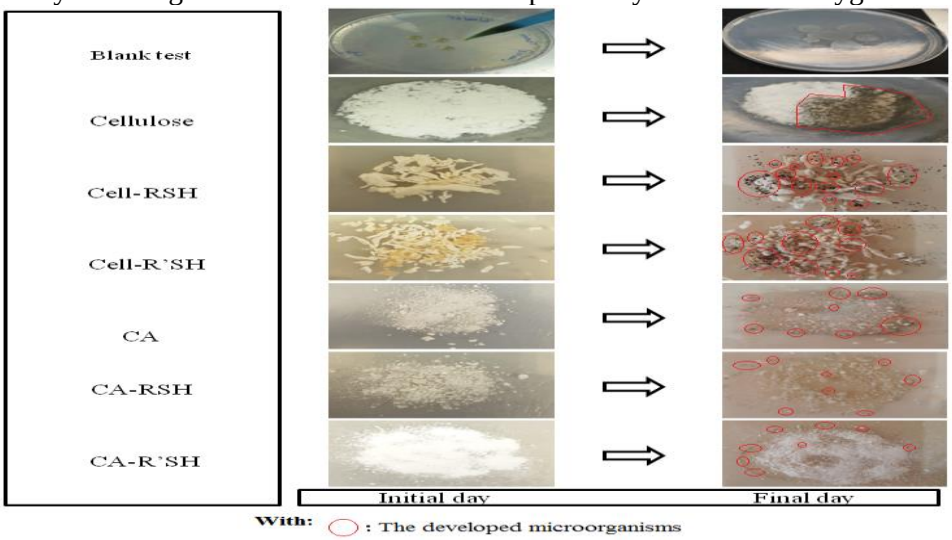

Figure 7: biodegradation tests under aerobic solid conditions of cellulose and its derivatives (Cell-RSH, Cell-R'SH, CA, CA-RSH and CA-R'SH) after 28 days of incubation

The quantification of the aerobic biodegradation process in liquid medium is assessed by measuring of biochemical oxygen demand (BOD) in a closed respirometer (ISO 14851 (1999)) during 40 days. Biodegradability values were expressed as the amount of O_2 consumed during biopolymer biodegradation per liter of culture medium (mg O_2/L). The amount of O_2 consumed in cellulose derivative's biodegradation process (after correction with the blank test) was expressed as a percentage of the theoretical oxygen demand (ThOD). The ThOD expressed as mass of O_2 per mass of polymer was determined by calculating the amount of O_2 necessary for aerobic mineralization of the cellulose derivatives, i.e., complete oxidation of C to CO_2.

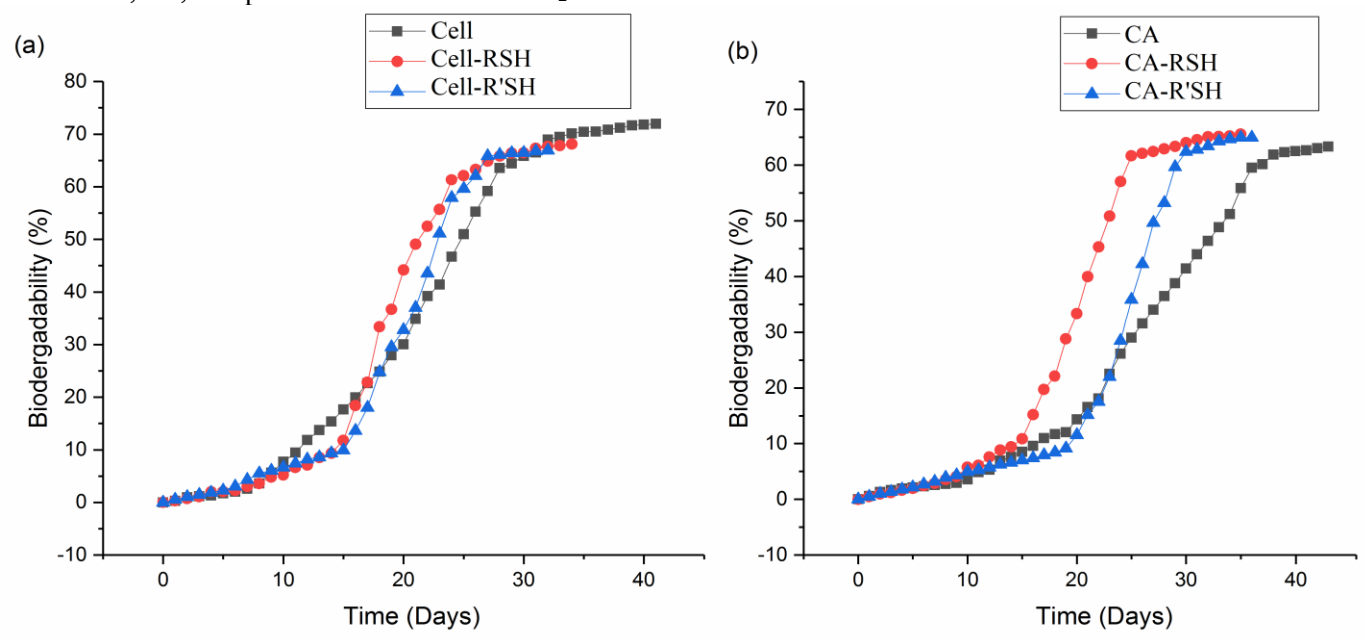

Figure 8: Biodegradation percentage of (a) cellulose, Cell-RSH, Cell-R'SH and (b) CA, CA-RSH and CA-R'SH after 40 days of incubation at 25°C under aerobic liquid conditions

According to the curves in Fig.8, it's noted that the latency time depends on the nature of the material and the composition of the lexivia. Furthermore, the appearance of the degradation process according to the curves obtained in Fig.8 is the same for all biopolymers. All biopolymers present almost the same pace of the degradation process. These curves are distinguished by a phase (around 8-10 days); this step may be due to the adaptation of the microorganisms to the new environment, by synthesizing the enzymes necessary for the biodegradation of the new carbon sources, and it may be assimilated to the lag phase of microbial growth. During the second phase, the biodegradation (BD) values increase exponentially of all the biopolymers. The microorganism's growth is due to the use of cellulose, CA and their derivatives as an only source of carbon. This phase can be generally modeled as an exponential equation in the following form:

$$BD = BD_0 e^{\mu t} \quad (6)$$

$$ln\, BD = \mu(t - t_0) + ln\, BD_0 \quad (7)$$

Where BD_0 represents the biodegradation at t_0, BD offers the biodegradation level at t and μ represents the rate of biodegradation. Then, at the last step a plateau phase was reached indicating that the biodegradation process takes end. This phase may be assimilated to the stationary phase of microbial growth, and may be due to the low concentration of nutrients, particularly the carbon sources (biopolymers). Biological oxygen demand (BOD) data obtained were expressed as a percentage of the theoretical oxygen demand (ThOD). The experimental results presented in figure 8 show that after 40 days on incubation (Fig.8a), the cellulose, Cell-RSH and Cell-R'SH were biodegraded respectively

over (71% - 67%); but, no signifigative differences were noted. Furthermore, in figure 8b, CA was biodegraded over 62% after 40 days of incubation and its derivatives (CA-RSH and CA-R'SH) showed the same level of biodegradation). The CA is also more biodegradable than its derivatives and also the cellulose is more biodegradable than CA. According to the table 3, it can be noted that the rates of biodegradation (μ) of Cell-RSH; Cell-R'SH and CA-RSH; CA-R'SH were greater than those of Cellulose and CA. Hence, the introduction of acrylic groups in cellulose and CA main chains increased significantly their biodegradation rate. Moreover, the incorporation of 2-hydroxyethyl methacrylate increased more their biodegradation rate than 2-methacrylic acid. The increase in biodegradation rate can be explained by the density of more ester groups along the chains, where microbial attack can occur by involving esterase enzymes. Fungi are known for their esterase production capacity on various plant polysaccharides [67]. This variation in biodegradation rate can also be explained by the variation of crystallinity index (CrI) from cellulose or CA to their derivatives. Moreover, it's known that biodegradation process is faster for amorphous than crystalline regions [68], for this reason the Cell-RSH, Cell-R'SH ,CA-RSH and CA-R'SH are more biodegradable than cellulose and CA. We can conclude that the lixivia and soil used as inoculum, have a remarkable biodegradation effect, and the growth of microorganisms is due to their ability to use these cellulose derivatives as a sole carbon source. The results obtained by the BOD method are mostly in agreement with those obtained by the microbial growth method.

Table 3: Rate of biodegradation (μ) of tested biopolymers

Biopolymers	Rate of biodegradation (μ)
Cell	0.11
Cell-RSH	0.23
Cell-R'SH	0.17
CA	0.12
CA-RSH	0.25
CA-R'SH	0.22

4. Conclusion

In conclusion, we have performed a comparative study on the behavior of acrylate-substituted cellulose and CA of different side chain length and nature groups. Two acrylates of cellulose (Cell-RSH and Cell-R'SH) and acrylates of CA (CA-RSH and CA-R'SH) respectively were successfully prepared by addition reaction between cellulose or CA and acrylic compounds using 1,6-HDI as a connecting agent. The chains to graft were attached to the backbone of the fibers using grafting to method and were lighted employing thiol-ene addition. The optimum conditions of the experiments were: grafting temperature 80°C, grafting time 3 h and homogenous medium. The chemical structures of the derivatives prepared were confirmed by NMR, FTIR, XRD and TGA analysis; also their solubility behaviors were established. The biodegradability of the cellulose, CA and their derivatives was confirmed by the standardized methods (ASTM, AFNOR, DIN and ISO). The results of biodegradation process indicated that the lixivia and soil used as inoculums, has a remarkable effect. The multiplication and growth of microorganisms and their ability to use these compounds as only carbon source was noted (in liquid medium and solid conditions). These materials emerged from raw resources can drive to wide game of applications in different industrial fields such as biofilms, bioplastics and biocomposites.

Acknowledgement:
The authors are grateful to Morocco CNRST - Program **PPR/2015/17-** (Rabat) for the support to carry out this work and laboratory associated contract.

References

[1] M. D. Teli and J. Sheikh, "Grafting of bamboo rayon with acrylic acid and its effect on cationic dyeing," *Cellul. Chem. Technol.*, vol. 46, pp. 53–59, 2012.
[2] M. Poletto, V. Pistor, and A. J. Zattera, "Structural Characteristics and Thermal Properties of Native Cellulose," in *Cellulose - Fundamental Aspects*, T. van de Ven and L. Godbout, Eds. 2013, pp. 54–68.
[3] H. P. S. A. Khalila *et al.*, "Production and modification of nanofibrillated cellulose using various mechanical processes: A review," *Carbohydr. Polym.*, vol. 106, pp. 207–213, 2014.
[4] G. Bogoeva-Gaceva *et al.*, "Natural Fiber Eco-Composites," *Polym. Polym. Compos.*, vol. 16, pp. 101–113, 2008.
[5] M. J. John and S. Thomas, "Biofibres and biocomposites," *Carbohydr. Polym.*, vol. 71, pp. 343–364, 2008.
[6] A. El Idrissi, S. El Barkany, H. Amhamdi, and A. K. Maaroufi, "Synthesis and characterization of the new cellulose derivative films based on the hydroxyethyl cellulose prepared from esparto 'stipa tenacissima' cellulose of Eastern Morocco. II. Esterification with acyl chlorides in a homogeneous medium," *J. Appl. Polym. Sci.*, vol. 127, pp. 3633–3644, 2013.
[7] S. Sen, J. D. Martin, and D. S. Argyropoulos, "Review of Cellulose Non-Derivatizing Solvent Interactions with Emphasis on Activity in Inorganic Molten Salt Hydrates," *ACS Sustain. Chem. Eng.*, vol. 1, p. 858−870, 2013.
[8] T. Heinze and T. Liebert, "Unconventional methods in cellulose functionalization," *Prog. Polym. Sci.*, vol. 26, pp. 1689–1762, 2001.
[9] I. Cumpstey, "Chemical Modification of Polysaccharides," *Hindawi Publ. Corp.*, 2013.
[10] C. R. Routray, B. Tosh, and N. Nayak, "Grafting of polymethyl methacrylate onto cellulose acetate in homogeneous medium using ceric (IV) ion as initiator," *Indian J. Chem. Technol.*, vol. 20, pp. 202–209, 2013.
[11] Y. Dong, L. I. Mosquera-Giraldo, L. S. Taylor, and K. J. Edgar, "Tandem Modification of Amphiphilic Cellulose Ethers for Amorphous Solid Dispersion via Olefin Cross-metathesis and Thiol-Michael Addition," *Polym. Chem.*, vol. 8, pp. 3129–3139, 2017.
[12] X. Qiu, S. Tao, X. Ren, and S. Hu, "Modified cellulose films with controlled permeatability and biodegradability by crosslinking with toluene diisocyanate under homogeneous conditions," *Carbohydr. Polym.*, vol. 88, pp. 1272–1280, 2012.
[13] L. Rueda *et al.*, "Isocyanate-rich cellulose nanocrystals and their selective insertion in elastomeric polyurethane," *Compos. Sci. Technol.*, vol. 71, pp. 1953–1960, 2011.
[14] D. Roy, M. Semsarilar, J. T. Guthrie, and S. Perrier, "Cellulose modification by polymer grafting : a review," *Chem. Soc. Rev.*, vol. 38, pp. 2046–2064, 2009.
[15] X. Samain, V. Langlois, E. Renard, and G. Lorang, "Grafting Biodegradable Polyesters onto Cellulose," *J. Appl. poly*, vol. 121, pp. 1183–1192, 2011.
[16] L. Wei and A. G. Mcdonald, "A Review on Grafting of Biofibers for Biocomposites," *Materials (Basel).*, vol. 9, pp. 1–23, 2016.
[17] A. Carlmark, E. Larsson, and E. Malmström, "Grafting of cellulose by ring-opening polymerisation - A review," *Eur. Polym. J.*, vol. 48, pp. 1646–1659, 2012.
[18] A. S. El-Khouly *et al.*, "Synthesis, characterization and antimicrobial activity of modified cellulose-graft-polyacrylonitrile with some aromatic aldehyde derivatives," *Carbohydr. Polym.*, vol. 83, pp. 346–353, 2011.

[19] D. Roy, J. S. Knapp, J. T. Guthrie, and S. Perrier, "Antibacterial cellulose fiber via RAFT surface graft polymerization," *Biomacromolecules*, vol. 9, pp. 91–99, 2008.
[20] J. Glasing, P. Champagne, and M. F. Cunningham, "Graft modification of chitosan, cellulose and alginate using reversible deactivation radical polymerization (RDRP)," *Curr. Opin. Green Sustain. Chem.*, vol. 2, pp. 15–21, 2016.
[21] D. Nystrom *et al.*, "Superhydrophobic and Self-Cleaning Bio-Fiber Surfaces via ATRP and Subsequent Postfunctionalization," *Appl. Mater. interfaces*, vol. 1, pp. 816–823, 2009.
[22] E. Larsson, S. A. Pendergraph, T. Kaldéus, E. Malmström, and A. Carlmark, "Cellulose Grafting by Photoinduced Controlled Radical Polymerisation," *Polym. Chem.*, vol. 6, pp. 1865–1874, 2015.
[23] A. Carlmark and E. Malmström, "Atom transfer radical polymerization from cellulose fibers at ambient temperature," *J. Am. Chem. Soc.*, vol. 124, pp. 900–901, 2002.
[24] N. Singh, Z. Chen, N. Tomer, S. R. Wickramasinghe, N. Soice, and S. M. Husson, "Modification of regenerated cellulose ultrafiltration membranes by surface-initiated atom transfer radical polymerization," *J. Memb. Sci.*, vol. 311, pp. 225–234, 2008.
[25] S. Li, M. Xiao, A. Zheng, and H. Xiao, "Cellulose microfibrils grafted with PBA via surface-initiated atom transfer radical polymerization for biocomposite reinforcement," *Biomacromolecules*, vol. 12, pp. 3305–3312, 2011.
[26] P. Chmielarz, "Cellulose-based graft copolymers prepared by simplified electrochemically mediated ATRP," *Express Polym. Lett.*, vol. 11, pp. 140–151, 2017.
[27] L. Bao, Y. Chen, W. Zhou, Y. Wu, and Y. Huang, "Bamboo Fibers @ Poly(ethylene glycol)-Reinforced Poly(butylene succinate) Biocomposites," *J. Appl. Polym. Sci.*, vol. 122, pp. 2456–2466, 2011.
[28] T. Meng, J. Zhang, J. He, Y. Zhang, X. Gao, and J. Yuan, "Graft copolymers prepared by atom transfer radical polymerization (ATRP) from cellulose," *Polymer (Guildf).*, vol. 50, no. 2, pp. 447–454, 2008.
[29] Y. Guo, X. Wang, Z. Shen, X. Shu, and R. Sun, "Preparation of cellulose-graft-poly(ε -caprolactone) nanomicelles by homogeneous ROP in ionic liquid," *Carbohydr. Polym.*, vol. 92, pp. 77–83, 2013.
[30] C. Routray and B. Tosh, "Graft copolymerization of methyl methacrylate (MMA) onto cellulose acetate in homogeneous medium: effect of solvent, initiator and homopolymer inhibitor," *Cellul. Chem. Technol.*, vol. 47, pp. 171–190, 2013.
[31] C. H. Worthley, K. T. Constantopoulos, M. Ginic-markovic, R. J. Pillar, J. G. Matisons, and S. Clarke, "Surface modification of commercial cellulose acetate membranes using surface-initiated polymerization of 2-hydroxyethyl methacrylate to improve membrane surface biofouling resistance," *J. Memb. Sci.*, vol. 385–386, pp. 30–39, 2011.
[32] Y. Shen, L. Dai, M.-F. Li, J. He, B. Wang, and R.-C. Sun, "Synthesis and comparison of graft copolymers using methacrylic monomers and cellulose via ATRP," *Cellul. Chem. Technol.*, vol. 48, pp. 653–660, 2014.
[33] Y. Kodama, M. Barsbay, and O. Güven, "Radiation-induced and RAFT-mediated grafting of poly (hydroxyethyl methacrylate) (PHEMA) from cellulose surfaces," *Radiat. Phys. Chem.*, vol. 94, pp. 98–104, 2014.
[34] T. Hajeeth, K. Vijayalakshmi, T. Gomathi, and P. N. Sudha, "Removal of Cu(II) and Ni(II) using cellulose extracted from sisal fiber and cellulose-g-acrylic acid copolymer," *Int. J. Biol. Macromol.*, vol. 62, pp. 59–65, 2013.
[35] A. E. Ofomaja, S. L. Ngema, and E. B. Naidoo, "The grafting of acrylic acid onto biosorbents: Effect of plant components and initiator concentration," *Carbohydr. Polym.*, vol. 90, pp. 201–209, 2012.
[36] V. K. Gupta, S. Agarwal, P. Singh, and D. Pathania, "Acrylic acid grafted cellulosic Luffa cylindrical fiber for the removal of dye and metal ions," *Carbohydr. Polym.*, vol. 98, pp. 1214–1221, 2013.
[37] A. Bessadok *et al.*, "Effect of chemical treatments of Alfa (Stipa tenacissima) fibres on water-sorption

properties," *Compos. Sci. Technol.*, vol. 67, pp. 685–697, 2007.
[38] T. Toledano-Thompson, M. I. Loría-Bastarrachea, and M. J. Aguilar-Vega, "Characterization of henequen cellulose microfibers treated with an epoxide and grafted with poly(acrylic acid)," *Carbohydr. Polym.*, vol. 62, pp. 67–73, 2005.
[39] E. S. Abdel-Halim, H. E. Emam, and M. H. El-Rafie, "Preparation and characterization of water soluble poly(acrylic acid)-hydroxypropyl cellulose composite," *Carbohydr. Polym.*, vol. 74, pp. 783–786, 2008.
[40] A. L. Buyanov, L. G. Revel'skaya, N. V. Bobrova, and G. K. Elyashevich, "New composite membranes based on crosslinked poly(acrylic acid) and porous polyethylene films," *Polym. Sci. - Ser. A*, vol. 48, no. 7, pp. 738–744, 2006.
[41] E. S. Abdel-Halim, "Preparation and characterization of poly(acrylic acid)-hydroxyethyl cellulose graft copolymer," *Carbohydr. Polym.*, vol. 90, pp. 930–936, 2012.
[42] A. Ben Mabrouk, H. Kaddami, S. Boufi, F. Erchiqui, and A. Dufresne, "Cellulosic nanoparticles from alfa fibers (Stipa tenacissima): extraction procedures and reinforcement potential in polymer nanocomposites," *Cellulose*, vol. 19, pp. 843–853, 2012.
[43] S. C. Ghanshyam, G. Lalit, and S. Rajeev, "Synthesis, characterization and metal ion sorption studies of graft copolymers of cellulose with glycidyl methacrylate and some comonomers," *Cellulose*, vol. 12, pp. 97–110, 2005.
[44] A. H. Zahran, J. L. Williams, and V. T. Stannett, "Radiation Grafting of Acrylic and Methacrylic Acid to Cellulose Fibers to Impart High Water Sorbency," *J. Appl. Polym. Sci.*, vol. 25, pp. 535–542, 1980.
[45] W. Dahou, D. Ghemati, A. Oudia, and D. Aliouche, "Preparation and biological characterization of cellulose graft copolymers," *Biochem. Eng. J.*, vol. 48, pp. 187–194, 2010.
[46] K. Littunen *et al.*, "Free radical graft copolymerization of nanofibrillated cellulose with acrylic monomers," *Carbohydr. Polym.*, vol. 84, pp. 1039–1047, 2011.
[47] J. Credou, R. Faddoul, and T. Berthelot, "One-step and eco-friendly modification of cellulose membranes by polymer grafting," *RSC Adv.*, vol. 4, pp. 60959–60969, 2014.
[48] G. S. Chauhan, R. Sharma, and H. Lal, "Synthesis and Characterization of Graft Copolymers of Hydroxypropyl Cellulose with Acrylamide and Some Comonomers," *J. Appl. Polym. Sci.*, vol. 91, pp. 545–555, 2004.
[49] M. K. Zahran and R. I. Mahmoud, "Peroxydiphosphate-metal ion-cellulose thiocarbonate redox system-induced graft copolymerization of vinyl monomers onto cotton fabric," *J. Appl. Polym. Sci.*, vol. 87, pp. 1879–1889, 2003.
[50] M. K. M. Z. Hyder and B. Ochiai, "Synthesis of a Selective Scavenger for Ag(I), Pd(II), and Au(III) Based on Cellulose Filter Paper Grafted with Polymer Chains Bearing Thiocarbamate Moieties," *Chem. Lett.*, vol. 46, pp. 492–494, 2017.
[51] B. V. Yu and S. W. Lee, "Synthesis of chemically active polymeric fibers bearing sulfo and carboxy groups," *Russ. J. Appl. Chem.*, vol. 80, no. 11, pp. 1918–1922, 2007.
[52] A. El Idrissi, S. El Barkany, H. Amhamdi, and A. K. Maaroufi, "Physicochemical characterization of celluloses extracted from Esparto 'stipa tenacissima' of Eastern Morocco," *J. Appl. Polym. Sci.*, vol. 128, pp. 537–548, 2013.
[53] P. Jandura, B. V.Kokta, and B. Riedl, "Fibrous Long-Chain Organic Acid Cellulose Esters and Their Characterization by Diffuse Reflectance FTIR Spectroscopy , Solid-State CP / MAS 13 C-NMR , and X-Ray Diffraction," *J. Appl. Polym. Sci.*, vol. 78, pp. 1354–1365, 2000.
[54] A. Calmon-Decriaud, V. Bellon-Maurel, and F. Silvestre, "Standard Methods for Testing the Aerobic Biodegradation of Polymeric Materials. Review and Perspectives," *Adv. Polym. Sci.*, vol. 135, pp. 207–226, 1998.

[55] A. Krzan, S. Hemjinda, S. Miertus, A. Corti, and E. Chiellini, “Standardization and certification in the area of environmentally degradable plastics,” *Polym. Degrad. Stab.*, vol. 91, pp. 2819–2833, 2006.

[56] J. Araki, T. Kataoka, N. Katsuyama, A. Teramoto, K. Ito, and K. Abe, “A preliminary study for fiber spinning of mixed solutions of polyrotaxane and cellulose in a dimethylacetamide/lithium chloride (DMAc/LiCl) solvent system,” *Polymer (Guildf).*, vol. 47, pp. 8241–8246, 2006.

[57] S. . Doyle and R. A. Pethrick, “Structure of fibrous cellulose acetate: X-ray diffraction, positron annihilation and electron microscopy investigations,” *J. Appl. Polym. Sci.*, vol. 33, no. 1, pp. 95–106, 1987.

[58] B. Boutevin, “From telomerization to living radical polymerization,” *J. Polym. Sci. Part A Polym. Chem.*, vol. 38, pp. 3235–3243, 2000.

[59] A. Gandini and M. N. Belgacem, “Modifying cellulose fiber surfaces in the manufacture of natural fiber composites,” in *Interface engineering of natural fibre composites for maximum performance*, Woodhead Publishing Limited, 2011, pp. 3–42.

[60] L. M. Wu, D. S. Tong, L. Z. Zhao, W. H. Yu, C. H. Zhou, and H. Wang, “Fourier transform infrared spectroscopy analysis for hydrothermal transformation of microcrystalline cellulose on montmorillonite,” *Appl. Clay Sci.*, vol. 95, pp. 74–82, 2014.

[61] H. S. Barud *et al.*, “Thermal behavior of cellulose acetate produced from homogeneous acetylation of bacterial cellulose,” *Thermochim. Acta*, vol. 471, pp. 61–69, 2008.

[62] C. Yin and X. Shen, “Synthesis of cellulose carbamate by supercritical CO2-assisted impregnation: Structure and rheological properties,” *Eur. Polym. J.*, vol. 43, pp. 2111–2116, 2007.

[63] A. G. Cunha *et al.*, “Bi-phobic cellulose fibers derivatives via surface trifluoropropanoylation,” *Langmuir*, vol. 23, pp. 10801–10806, 2007.

[64] G. R. Filho, S. F. da Cruz, D. Pasquini, D. A. Cerqueira, V. de S. Prado, and R. M. N. de Assunção, “Water flux through cellulose triacetate films produced from heterogeneous acetylation of sugar cane bagasse,” *J. Memb. Sci.*, vol. 177, pp. 225–231, 2000.

[65] W. Hu, S. Chen, Q. Xu, and H. Wang, “Solvent-free acetylation of bacterial cellulose under moderate conditions,” *Carbohydr. Polym.*, vol. 83, pp. 1575–1581, 2011.

[66] P. A. Dantas and V. R. Botaro, “Synthesis and Characterization of a New Cellulose Acetate-Propionate Gel: Crosslinking Density Determination,” *Open J. Polym. Chem.*, vol. 2, pp. 144–151, 2012.

[67] P. Biely, “Microbial carbohydrate esterases deacetylating plant polysaccharides,” *Biotechnol. Adv.*, vol. 30, pp. 1575–1588, 2012.

[68] N. Jiang, L. Zhao, and Z. Gan, “Influence of nucleating agent on the formation and enzymatic degradation of poly (butylene adipate) polymorphic crystals,” *Polym. Degrad. Stab.*, vol. 95, pp. 1045–1053, 2010.